Temperature dependence of Raman spectra for individual silicon nanowires

Gregory S. Doerk, Carlo Carraro, and Roya Maboudian
Department of Chemical Engineering, University of California, Berkeley, California 94720, USA
(Received 6 May 2009; revised manuscript received 12 July 2009; published 27 August 2009)

The temperature dependence of the Stokes first-order optical phonon frequency has been measured for individual silicon nanowires with diameters between 33 to 180 nm in the temperature range of 20 to 300 °C. The nanowires were synthesized via both the vapor-liquid-solid method and electrochemical etching of bulk silicon. Significant laser-induced local heating was avoided by using a laser power of 0.5 mW or less, corresponding to fluxes of ≤ 0.7 mW/μm^2. For both types of nanowires the slope of Raman frequency vs temperature closely matches the value of bulk Si, $(\frac{d\omega}{dT}) = -0.022 \pm .001$ cm^{-1} °C^{-1}, across the entire diameter range, indicating no change in lattice anharmonicity. These results have important implications for understanding nanowire lattice thermal conductivity and extending the domain for Raman thermometry of silicon nanostructures.

DOI: 10.1103/PhysRevB.80.073306 PACS number(s): 78.30.Am, 63.22.Gh, 65.80.+n, 81.70.Fy

Semiconductor nanowires are promising for integration into thermoelectric materials as they may reduce lattice thermal conductivity while maintaining high electrical conductivity.[1] Single-crystal silicon nanowires (NWs) grown by the vapor-liquid-solid process (VLS) for instance, show a strong dependence of thermal conductivity on diameter, which has been attributed to boundary scattering.[2] More recently it was demonstrated that single-crystal silicon nanowires synthesized by Ag-catalyzed electrochemical etching of Si wafers possess thermal conductivities five to eight times lower than those of VLS Si NWs of the same diameter, enabling orders of magnitude improvement over bulk Si in the thermoelectric figure of merit.[3] These surprising results were attributed to the rough surfaces of the electrochemically etched (EE) Si NWs, though the available theories for determining thermal conductivity of crystalline materials that account for surface roughness could not provide quantitative agreement with the experimental data.[4,5]

As a probe of phonons in crystals, Raman spectrometry may provide valuable insight into their thermal properties. Specifically, the anharmonicity of the vibrational potential energy provides a route to precisely measure local temperature in the crystal through Raman spectrometry.[6] Previous Raman investigations done on ensembles of Si NWs with small diameters ($D \lesssim 20$ nm) have assumed bulk anharmonic behavior in order to isolate the effects of quantum confinement.[7–9] Yet one report has claimed anharmonic constants relating the temperature dependence of the first-order optical phonon frequency from an ensemble of ~20 nm diameter Si NWs that are different from those for bulk Si.[10] Therefore, it is unclear whether anharmonic constants for silicon nanowires change with decreasing diameter and at what diameter this becomes significant.

Furthermore, in the case of EE Si NWs, recent theoretical modeling of roughened Si NWs indicate the need to include the entire phonon frequency range in calculations.[11,12] In particular, disordered surfaces may substantially decrease the lifetime of propagating modes (by at least one order of magnitude), and result in a larger proportion of heat being transmitted via higher frequency (~70 cm^{-1}), nonpropagating, diffusive (including optical) modes similar to those in amorphous Si.[12] To date there have been no temperature related Raman studies of EE Si NWs, which would potentially aid in the clarification and verification of emerging models for heat transfer in roughened nanostructures, and will improve our understanding of the behavior of their high-frequency phonons in general.

In this Brief Report we study the temperature dependence of the Raman spectra of individual VLS Si NWs with diameters in the range of about $\simeq 30$ to $\simeq 180$ nm and of EE Si NWs with diameters in the range of about $\simeq 50$ to $\simeq 130$ nm, in the temperature ranges of 20–250 °C and 20–300 °C, respectively.

The growth of VLS Si NWs was achieved by Au-catalyzed atmospheric pressure chemical vapor deposition following the procedure described previously.[13] A key feature is that the Au catalyst was deposited as a film via galvanic displacement from potassium tetrachloroaurate ($KAuCl_4$).[14,15] Inhomogeneous dewetting and alloying of the Au film with the Si substrate immediately before growth results in a dense NW array with a broad diameter distribution,[16–18] and Si NWs greater than 30 nm in diameter grow preferentially in the [111] crystallographic direction.[19] A scanning electron microscope (SEM) image of as-synthesized VLS Si NWs is shown in Fig. 1(a).

Electrochemically etched Si NWs were synthesized directly following the methods of Ref. 3, originally demonstrated by Peng *et al.*[20,21] Briefly, *n* type ($\rho = 1-5$ Ω cm) single-crystal on-axis Si(111) dice were sonicated in acetone and isopropyl alcohol, rinsed with DI H_2O, and dried in N_2. The sample dice were then immersed in a solution of 40 mM $AgNO_3$ and 5 M HF for 2 h or less, at an etch rate of approximately 5 μm/hr. After etching, the samples were rinsed with deionized (DI) H_2O to remove Ag dendrites that grow during the etching process, and immersed into concentrated nitric acid for at least one hour to remove any remaining Ag. Finally, the samples were immersed in concentrated HF for 1 min to remove any SiO_2. Figure 1(b) shows an SEM image of as-synthesized EE Si NWs.

Wires were dispersed from suspension in ethanol onto Si(111) dice, each covered with an evaporated tungsten film to mask the substrate. Since both the wires synthesized by

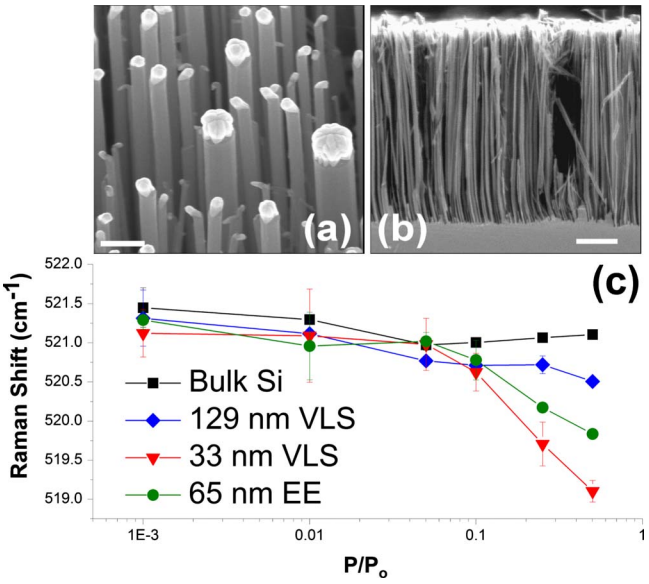

FIG. 1. (Color online) (a)–(b) Scanning electron micrographs of as-synthesized Si NWs: (a) VLS grown Si NWs (30° tilt, scale bar=1 μm), (b) cross-sectional image of Si NWs from electrochemical etching of Si(111) substrates (scale bar=2 μm). (c) Calibration for determination of local heating effect vs relative laser power (log scale) in VLS and EE Si NWs by measurement of the Raman shift of the optical phonon peak. The clear redshifts above a relative laser power of 0.05 for the 33 nm diameter VLS wire and the 65 nm diameter EE wire indicate the onset of significant local heating that skews the wire temperature to higher values than the underlying substrate.

VLS epitaxy using $SiCl_4$ and the EE wires are straight, the wires layed flat on the film surface, maintaining good thermal contact. Tungsten was chosen because it is thermally and chemically stable, and forms no silicides below temperatures of 550 °C.[22] A portion of the substrate was covered during the evaporation so that the bulk silicon would be exposed in that region only. Raman spectrometry (JYHoriba LabRAM) was performed in backscattering configuration with an excitation line provided by a HeNe laser (632.8 nm wavelength) through an Olympus BX41 100X confocal microscope (numerical aperture=0.8; laser spot size <1 μm). Samples were heated on a homebuilt resistive heating stage and were studied in room atmosphere. Due to the good contact with the substrate, the temperature of the nanowires was taken to be the same as the temperature of the substrate, which was measured via the exposed Si section using the Stokes-antiStokes intensity ratio according to the relation

$$\frac{I_S}{I_{AS}} = A\left(\frac{\omega_S}{\omega_{AS}}\right)^3 \exp\left(\frac{hc\omega}{k_B T}\right) \quad (1)$$

where ω_S and ω_{AS} are the frequency of the stokes and anti-Stokes photons, h is Planck's constant, c is the speed of light, ω is the phonon frequency (in cm^{-1}), k_B is Boltzmann's constant, T is absolute temperature, and A is a constant determined by the absorption constants and Raman cross sections at the Stokes and antiStokes frequencies that must be calibrated for the sample.[6] The parameter A was measured as 0.96 for the Si substrate at room temperature and assumed constant for the range of temperatures studied. Due to the large polarization anisotropy in nanowires that arises from the dielectric constant mismatch between the nanowire and air,[23] wires were aligned along the laser polarization direction to maximize the intensity of the Raman spectra.

In order to properly probe the temperature response of individual silicon nanowires, the laser power must be large enough for accurate resolution of the Stokes and antiStokes peaks, but not too large so that local heating renders the assumption of near-thermal equilibrium with the substrate invalid. The Stokes to antiStokes peak ratio for the first-order optical phonon has been previously used to estimate local temperature according to Eq. (1), and it is convenient in that it is not influenced by extraneous factors such as stress, doping, and confinement. However, there is no guarantee that the prefactor "A" is the same for any sized nanowire as for bulk Si, and accurate determination of I_{AS}/I_S becomes increasingly difficult as wire diameter and laser power are decreased. To circumvent the problem of high error in the I_{AS}/I_S ratio for smaller nanowires, the Stokes first-order optical Raman shift, which redshifts with increasing temperature due to lattice anharmonicity, was directly measured as a function of filtered laser power relative to the full laser power (the full, unfiltered power is approximately 10 mW at the sample). The power at which local heating is acceptably low is designated as the point in which the Raman shift plateaus at a constant value, as shown in Fig. 1(c). The Raman shift of bulk Si does not decrease below 521 cm^{-1}, the expected room-temperature value which indicates no local heating, while the 129 nm diameter wire Raman shift decreases minimally ($\sim$0.8 cm^{-1} over the entire power range). The onset of local heating above a relative laser power of 0.05 is clearly seen by the decrease in Raman shift of $\sim$1.2 cm^{-1} for a 65 nm EE wire, and a decrease in Raman shift of $\sim$1.9 cm^{-1} for a the 33 nm VLS wire, the smallest wire studied in this report. Similar results were obtained for the other wires studied. Therefore, the temperature response for all VLS wires in this study was performed at relative laser powers of 0.05 (approximately 0.5 mW or 0.7 $mW/\mu m^2$) or less.

Phonon anharmonicity is reflected in the temperature dependence of the Raman peak position and its full width at half maximum. For individual nanowires, the latter is rather imprecise due to large variability in absolute peak intensity arising from experimental factors such as correct focus and position of the laser spot. Therefore, we restrict our study to the temperature dependence of the peak position. The Raman frequency is given by

$$\omega(T) = \omega_o + \Delta_{TE}(T) + \Delta_A(T) \quad (2)$$

where ω_o is the frequency at 0 K, $\Delta_{TE}(T)$ is the frequency shift due to thermal expansion, and $\Delta_A(T)$ is the frequency shift due to anharmonic phonon-phonon coupling.[24] Above room temperature the relationship between Raman shift and temperature is typically linear. Expanding expressions for the thermal expansion[24] and anharmonic coupling[6] effects in a

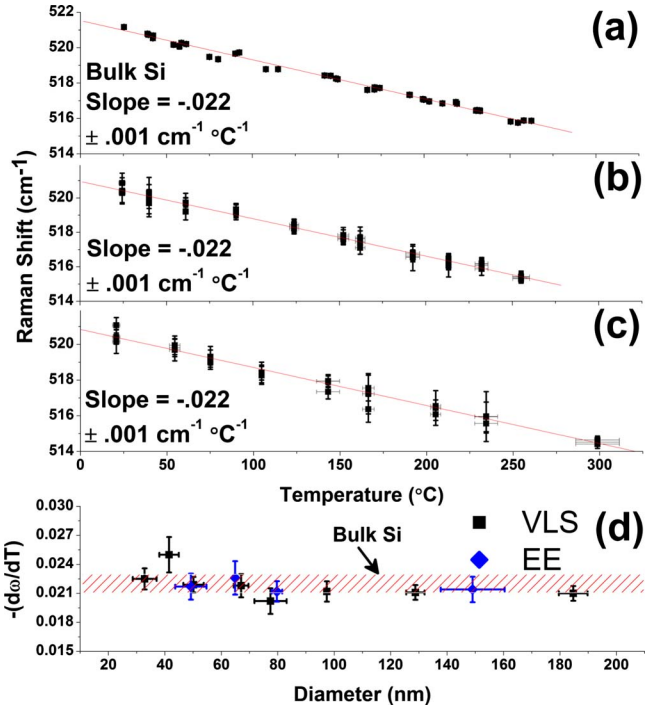

FIG. 2. (Color online) Temperature dependence of the optical phonon frequency for: (a) a bulk silicon sample, (b) a 50 nm VLS Si NW, and (c) a 50 nm EE Si NW. The insets in (b) and (c) are SEM images of each respective wire (scale bars=500 nm). (c) Slope of optical phonon Raman shift vs temperature for VLS Si NWs ranging in diameter from 33 to 185 nm and for EE Si NWs ranging in diameter from 50 to 150 nm. They are all scattered around the value for bulk silicon, with no apparent trend with diameter, indicating that the slopes are all equal to the bulk silicon value after accounting for experimental error.

Maclaurin series and cutting off at linear terms, the slope for this relationship is given approximately by:

$$\left(\frac{d\omega}{dT}\right) \approx -3\omega_o \gamma\alpha + \frac{k_B}{hc\omega_o}[4A + 9B] \tag{3}$$

where γ is the Gruneisen parameter, α is the coefficient of linear thermal expansion, and A and B are the cubic and quartic anharmonic constants, respectively.[6]

As a result, our data for Raman shift vs temperature are fit with straight lines. Since other anharmonic contributions dominate over thermal expansion,[25] a difference in the slope of this line would indicate different anharmonic constants. Figure 2(a) is a plot of Raman shift versus T for the underlying bulk Si substrate. Linear regression analysis yields a slope for $(\frac{d\omega}{dT}) = -0.022 \pm .001$ cm^{-1} °C^{-1}, which is in good agreement with previous reports that give a value of $(\frac{d\omega}{dT}) \approx -0.024$ cm^{-1} °C.[24–26] The discrepancy may arise from the more limited range of temperature used in our experiment and the assumption of a constant prefactor in Eq. (1) over the full temperature range. However, concerning the anharmonicity of Si NWs, it is important to compare direct measurements made in the same manner. Figure 2(b) shows the dependence on temperature of the optical Raman shift of a 50 nm VLS wire, for which linear regression gives a value for $(\frac{d\omega}{dT})$ of $-0.022 \pm .001$ cm^{-1} °C^{-1}. Similarly, linear regression of the optical Raman shift dependence on temperature for a ~50 nm EE NW, shown in Fig. 2(c), yields a slope of $-0.022 \pm .001$ cm^{-1}. These values for $(\frac{d\omega}{dT})$ are equivalent to the bulk Si value, indicating no change in the anharmonic constants for these nanowires compared to bulk Si. In fact, as shown in Fig. 2(d) the temperature dependence of the Raman spectra is nearly the same as for bulk Si across the range of NW diameters examined, with no trend apparent.

Anharmonic contributions may dramatically effect lattice thermal conductivity. For example, strong anharmonic coupling between guest and host atom vibrational modes is believed to be responsible for the glasslike thermal conductivity in crystalline clathrate compounds.[27,28] Since typical treatments of surface roughness cannot account for the lower thermal conductivity of EE Si NWs, factors such as boundary-induced adjustments in the effective lattice anharmonicity of the EE Si NWs may play a role and provide a possible explanation. In light of the surprisingly low thermal conductivity of a ~50 nm EE NW in Ref. 3 that approaches the amorphous limit, the above results are of particular interest. While heat is believed to be transported primarily by lower frequency acoustic phonons,[29] it has recently been suggested that accurate quantitative description of the thermal conductivity in semiconductors requires inclusion of the anharmonic optical phonon decay to acoustic phonons.[30,31]

Thus, a change in the anharmonicity of optical phonons or higher-frequency acoustic phonons in nanowires could then help account for reductions in heat transport beyond those described through boundary scattering alone. We have performed measurements of the temperature dependence of the 2TA peak in the vicinity of 300 cm^{-1} for a 80 nm EE wire and a 77 nm VLS wire yielding slopes of -0.0133 ± 0.003 cm^{-1} °C^{-1} and -0.0135 ± 0.002 cm^{-1} °C^{-1}, respectively. These values are nearly identical to that measured for bulk Si, -0.0132 ± 0.001 cm^{-1} °C^{-1}, indicating that bulk silicon anharmonicity is retained for this two-phonon acoustic interaction as well. Therefore, we infer that lattice anharmonicity cannot play a significant role in the severely depressed thermal conductivity in roughened EE Si nanowires compared with smooth-surfaced VLS Si nanowires.

In summary, we have performed detailed measurements of the temperature dependence of the optical phonon frequency in Raman spectra for individual single-crystal silicon nanowires synthesized by vapor-liquid-solid growth and electrochemical etching in the temperature range of 20 to 300 °C. For VLS nanowires down to 33 nm in diameter, and EE nanowires down to 49 nm in diameter this temperature dependence matches the linear temperature dependence found in bulk single-crystal silicon, indicating no change in lattice anharmonicity for the nanowires in this diameter range. These results strongly rule out lattice anharmonicity effects as the cause of thermal conductivity reduction in EE Si NWs. Furthermore, they verify the straightforward extension of noncontact temperature measurements from bulk silicon structures to silicon nanowires with variable surface morphology using Raman spectrometry. This is particularly valuable considering the ubiquitous presence of silicon in current and emerging nanotechnology and the increasing use

of Raman spectrometry for measurements of thermal transport in nanostructures, as evidenced by recent experimental studies using Raman spectrometry to measure heat in current-carrying molecular junctions[32] and thermal transport in single-walled carbon nanotubes.[33]

We acknowledge Nicola Ferralis for the help with the Raman setup and for useful discussions. This work was supported by the National Science Foundation under Grant No. EEC-0425914 (Center of Integrated Nanomechanical Systems) and Grant No. DMR-0804646.

[1] D. Li, S. Huxtable, A. Abramson, and A. Majumdar, J. Heat Transfer **127**, 108 (2005).
[2] D. Li, Y. Wu, P. Kim, L. Shi, P. Yang, and A. Majumdar, Appl. Phys. Lett. **83**, 2934 (2003).
[3] A. Hochbaum, R. Chen, R. Delgado, W. Liang, E. Garnett, M. Najarian, A. Majumdar, and P. Yang, Nature (London) **451**, 163 (2008).
[4] N. Mingo, L. Yang, D. Li, and A. Majumdar, Nano Lett. **3**, 1713 (2003).
[5] A. Moore, S. Saha, R. Prasher, and L. Shi, Appl. Phys. Lett. **93**, 083112 (2008).
[6] M. Balkanski, R. F. Wallis, and E. Haro, Phys. Rev. B **28**, 1928 (1983).
[7] R. Gupta, Q. Xiong, C. Adu, U. Kim, and P. Eklund, Nano Lett. **3**, 627 (2003).
[8] S. Piscanec, M. Cantoro, A. C. Ferrari, J. A. Zapien, Y. Lifshitz, S. T. Lee, S. Hofmann, and J. Robertson, Phys. Rev. B **68**, 241312(R) (2003).
[9] Z. Su, J. Sha, G. Pan, J. Liu, D. Yang, C. Dickinson, and W. Zhou, J. Phys. Chem. B **110**, 1229 (2006).
[10] Y. Chen, B. Peng, and B. Wang, J. Phys. Chem. C **111**, 5855 (2007).
[11] P. Martin, Z. Aksamija, E. Pop, and U. Ravaioli, Phys. Rev. Lett. **102**, 125503 (2009).
[12] D. Donadio and G. Galli, Phys. Rev. Lett. **102**, 195901 (2009).
[13] G. Doerk, N. Ferralis, C. Carraro, and R. Maboudian, J. Mater. Chem. **18**, 5376 (2008).
[14] C. Carraro, R. Maboudian, and L. Magagnin, Surf. Sci. Rep. **62**, 499 (2007).
[15] L. Magagnin, R. Maboudian, and C. Carraro, J. Phys. Chem. B **106**, 401 (2002).
[16] D. Gao, R. He, C. Carraro, R. Howe, P. Yang, and R. Maboudian, J. Am. Chem. Soc. **127**, 4574 (2005).
[17] N. Ferralis, R. Maboudian, and C. Carraro, J. Phys. Chem. C **111**, 7508 (2007).
[18] N. Ferralis, R. Maboudian, and C. Carraro, J. Am. Chem. Soc. **130**, 2681 (2008).
[19] I. Lombardi, A. Hochbaum, P. Yang, C. Carraro, and R. Maboudian, Chem. Mater. **18**, 988 (2006).
[20] K. Peng, Y. Yang, S. Gao, and J. Zhu, Adv. Mater. **14**, 1164 (2002).
[21] K. Peng, Y. Yang, S. Gao, and J. Zhu, Adv. Funct. Mater. **13**, 127 (2003).
[22] Y. Pauleau, F. Dassapa, P. Lami, J. Oberlin, and F. Romagna, J. Mater. Res. **4**, 156 (1989).
[23] J. Frechette and C. Carraro, Phys. Rev. B **74**, 161404(R) (2006).
[24] H. H. Burke and I. P. Herman, Phys. Rev. B **48**, 15016 (1993).
[25] J. Menendez and M. Cardona, Phys. Rev. B **29**, 2051 (1984).
[26] V. Brazhkin, S. Lyapin, I. Trojan, R. Voloshin, A. Lyapin, and N. Mel'nik, JETP Lett. **72**, 195 (2000).
[27] J. Tse, D. Klug, J. Zhao, W. Sturhahn, E. Alp, J. Baumert, C. Gutt, M. Johnson, and W. Press, Nature Mater. **4**, 917 (2005).
[28] M. Christensen, A. Abrahamsen, N. Christensen, F. Juranyi, N. Andersen, K. Lefmann, J. Andreasson, C. Bahl, and B. Iversen, Nature Mater. **7**, 811 (2008).
[29] G. Srivastava, J. Phys. Chem. Solids **41**, 357 (1980).
[30] M. Kazan, S. Pereira, J. Coutinho, M. Correia, and P. Masri, Appl. Phys. Lett. **92**, 211903 (2008).
[31] M. Kazan, S. Pereira, M. R. Correia, and P. Masri, Phys. Rev. B **77**, 180302(R) (2008).
[32] Z. Ioffe, T. Shamai, A. Ophir, G. Noy, I. Yutsis, K. Kfir, O. Cheshnovsky, and Y. Selzer, Nat. Nanotechnol. **3**, 727 (2008).
[33] I. Hsu, R. Kumar, A. Bushmaker, S. Cronin, M. Pettes, L. Shi, T. Brintlinger, M. Fuhrer, and J. Cumings, Appl. Phys. Lett. **92**, 063119 (2008).